

TnT - The Normalized Transformer: Eigen-Learning Rates Meet Stepwise Normalization

Anonymous ACL submission

Abstract

Traditional Transformer architectures process input sequences through self-attention mechanisms and feed-forward networks operating in Euclidean space. However, this representation may not fully capture the complex, hierarchical relationships inherent in structured data. To address this limitation, we introduce N Transformer, an enhanced encoder-decoder architecture that applies normalization to all embeddings, attention mechanisms, and hidden states to maintain unit norm. N-Transformer ensures that token representations traverse the surface of a hypersphere with each layer contributing a displacement towards the target output predictions. These displacements are defined by the MLP and attention blocks, whose vector components also reside on the same hypersphere. Our experiments demonstrate that N-transformer achieves superior performance compared to standard transformer architectures within a comparable parameter range. Through our experiments we show that N-transformer has superior performance compared to standard transformer architectures on the same parameter scale. Furthermore, N-transformer achieves an average 11.31% improvement on GLUE tasks and great improvements on the SuperGLUE tasks, 11.5% on WiC and 3.79% on BoolQ. Additionally, pre-training experiments on the OpenWebText dataset reveal a 7% lower validation loss than the baseline transformer model after the same number of training iterations.

1 Introduction

The transformer (Vaswani et al., 2017) architecture has become the foundation of modern natural language processing, with numerous variants proposed to enhance its capabilities across different tasks. While much research has focused on architectural modifications like attention mechanisms and positional encodings such as RoPE(Su et al., 2024), the role of normalization in these models

remains an active area of investigation. It has been observed that applying various normalization techniques is beneficial (Salimans and Kingma, 2016), leading to experiments incorporating normalization layers such as LayerNorm (Ba, 2016) and RMSNorm (Zhang and Sennrich, 2019) at nearly every possible position within the network (Xiong et al., 2020).

Another approach to the model normalization is through controlling the norm of weights using weight decay (Loshchilov, 2017). Recent studies (D’Angelo et al., 2023) suggest reevaluating the role of weight decay and taking a closer look at rotations rather than focusing solely on vector norms (Kodryan et al., 2022).

The recently released nGPT paper by NVIDIA (Loshchilov et al., 2024) serves as a major source of inspiration for our work. We extend the functionality of the methodology outlined in their technical report by implementing a Normalized encoder-decoder architecture with representation learning on the hypersphere.

We define the Normalized Transformer (N-transformer), which incorporates normalization throughout the architecture to ensure all computations occur on the unit hypersphere. Previous approaches apply normalization primarily for training stability, N-transformer uses normalization as a fundamental design principle that shapes how the model processes and transforms sequences. By constraining embeddings, attention matrices, and hidden states to unit norm, it creates a more structured optimization landscape where each layer’s transformations are naturally bounded and interpretable as movements along the hypersphere. The key technical innovation lies in its reformulation of the standard Transformer blocks. Rather than applying unrestricted linear transformations followed by non-linearities, the attention and feed-forward layers compute normalized displacements that preserve the hyperspherical constraint.

| Standard Transformer | N-transformer |
|--|--|
| $h_A \leftarrow \text{ATTN}(\text{RMSNorm}(h))$ | $h_A \leftarrow \text{ATTN}(h)$ with normalized Q, K scaled by s_{qk} |
| $h \leftarrow h + h_A$ | $h \leftarrow \mathcal{N}(\mathcal{N}(h) + \alpha_A(\mathcal{N}(h_A) - \mathcal{N}(h)))$ |
| $h_C \leftarrow \text{CROSS}(\text{RMSNorm}(h))$ | $h_C \leftarrow \text{CROSS}(h)$ with normalized Q, K scaled by s_{qk} |
| $h \leftarrow h + h_C$ | $h \leftarrow \mathcal{N}(\mathcal{N}(h) + \alpha_C(\mathcal{N}(h_C) - \mathcal{N}(h)))$ |
| $h_M \leftarrow \text{MLP}(\text{RMSNorm}(h))$ | $h_M \leftarrow \text{MLP}(h)$ with scaled intermediate states s_{uv} |
| $h \leftarrow h + h_M$ | $h \leftarrow \mathcal{N}(\mathcal{N}(h) + \alpha_M(\mathcal{N}(h_M) - \mathcal{N}(h)))$ |
| Final: $h \leftarrow \text{RMSNorm}(h)$ | No final normalization needed |
| Parameters unconstrained | All matrices and embeddings normalized along embedding dimension after each batch |

Table 1: Transformer vs. N-transformer Architecture Comparison where $\mathcal{N}(\cdot)$ represents L2 normalization. $\alpha_A, \alpha_C, \alpha_M$ are learnable update rates for attention, cross-attention, and MLP respectively. s_{qk} is the learned scaling for query-key interactions. s_{uv} is the learned scaling for MLP intermediate states.

Our contributions are as follows:

- Unified Normalization in Encoder-Decoder Architecture:** We normalize all vectors that form the embedding dimensions of network matrices to lie on a unit norm hypersphere. This operation converts matrix vector products into cosine similarities, limiting the range to $[-1, 1]$. The normalization renders weight decay unnecessary. Our approach maintains normalized representations throughout the information flow, including the cross-attention mechanism. This unified approach reduces the parameter count by 2.5%.
- Adaptive Scaling Mechanism for Component Integration:** We introduce learnable eigen learning rates for both encoder and decoder components. These scaling factors automatically balance the contributions of self-attention, cross-attention, and feed-forward networks, allowing the model to dynamically adjust the importance of each component during training.
- Faster Convergence:** The N-transformer model demonstrates faster convergence, attaining a lower validation loss compared to the standard transformer model for the same number of training iterations, indicating more efficient optimization.

2 Design and Architecture Details

This section outlines the baseline Transformer and the modifications necessary to derive its normalized

version.

2.1 Self Attention

The self-attention mechanism in N-transformer builds upon traditional transformer architectures while introducing normalization-based optimizations for both encoder and decoder components.

2.1.1 Standard Transformer Self-Attention

In the standard Transformer, self-attention operates on an input sequence $X \in \mathbb{R}^{B \times T \times D}$, where B is the batch size, T is the sequence length, and D is the embedding dimension. The attention mechanism is computed as:

$$\text{Attention}(Q, K, V) = \text{softmax}\left(\frac{QK^T}{\sqrt{d_k}}\right)V \quad (1)$$

where Q, K , and V are linear projections of the input:

$$Q = XW_Q \quad K = XW_K \quad V = XW_V \quad (2)$$

2.1.2 N-transformer Self-Attention

The N-transformer modifies this mechanism by introducing normalized query and key representations:

$$\text{normalized}(x) = \frac{x}{|x|_2} \quad (3)$$

The modified attention computation becomes:

$$Q_{\text{norm}} = s_{qk} \cdot \text{normalized}(Q) \quad (4)$$

$$K_{\text{norm}} = s_{qk} \cdot \text{normalized}(K) \quad (5)$$

140 where s_{qk} is a learned scaling parameter initialized
141 as:

$$142 \quad s_{qk} = \frac{1}{\sqrt{D}} \cdot s_{\text{init}} \quad (6)$$

143 The attention scores are computed by taking the
144 dot product of the query and key vectors, scaling
145 by $\frac{1}{\sqrt{d_k}}$, and applying a softmax function to obtain
146 attention weights. A masking matrix M prevents
147 attending to future tokens, ensuring causal attention:
148

$$149 \quad \text{Attention}(\mathbf{q}, \mathbf{k}, \mathbf{v}) = \text{softmax} \left(\frac{\mathbf{q}\mathbf{k}^\top}{\sqrt{d_k}} + M \right) \mathbf{v}. \quad (7)$$

150 Multi-head attention is implemented using sepa-
151 rate projections for each attention head, with results
152 concatenated and projected back to the model's di-
153 mension:

$$154 \quad \mathbf{h}_A = \text{Concat}(\text{head}_1, \dots, \text{head}_{n_{\text{heads}}})W_O. \quad (8)$$

155 2.2 Cross-Attention Mechanism

156 Cross-attention is employed within the encoder-
157 decoder framework to enable interactions between
158 the encoder's contextual representations and the
159 decoder's token embeddings. Unlike self-attention,
160 which operates within a single sequence, cross-
161 attention allows the decoder to attend to the en-
162 coder's output, making it essential for tasks such
163 as sequence-to-sequence learning. Given the en-
164 coder's output hidden states $E \in \mathbb{R}^{B \times S \times D}$ and the
165 decoder's current hidden states $H_d \in \mathbb{R}^{B \times T \times D}$,
166 cross-attention enables the decoder to selectively
167 focus on relevant parts of the input sequence during
168 generation.

169 2.2.1 Standard Transformer Cross-Attention

170 In the standard Transformer, cross-attention com-
171 putes queries from the decoder's hidden states
172 while deriving keys and values from the encoder's
173 output:

$$174 \quad \text{CrossAttention}(Q_d, K_e, V_e) = \\ 175 \quad \text{softmax} \left(\frac{Q_d K_e^T}{\sqrt{d_k}} \right) V_e \quad (9)$$

176 This mechanism allows each decoder position
177 to attend to all encoder positions, creating a direct
178 information pathway between the input and output
179 sequences.

180 2.2.2 N-transformer Cross-Attention

181 The N-transformer enhances cross-attention by ap-
182 plying the same normalization principles used in
183 self-attention. This modification ensures consis-
184 tent scale management throughout the network and
185 stable gradient flow between encoder and decoder.
186 The normalized queries and keys are computed as:

$$187 \quad Q_{d,\text{norm}} = s_{qk} \cdot \text{normalized}(Q_d) \quad (10)$$

$$188 \quad K_{e,\text{norm}} = s_{qk} \cdot \text{normalized}(K_e) \quad (11)$$

189 where the scaling factor s_{qk} maintains the same
190 initialization as in self-attention. The final cross-
191 attention computation becomes:

$$193 \quad \text{CrossAttention}(Q_d, K_e, V_e) = \\ 194 \quad \text{softmax} \left(\frac{Q_{d,\text{norm}} K_{e,\text{norm}}^T}{\sqrt{d_k}} \right) V_e \quad (12)$$

195 This normalized cross-attention ensures that the
196 interaction between encoder and decoder represen-
197 tations occurs in a well-conditioned space, poten-
198 tially leading to more stable training and better
199 convergence.

200 2.3 MLP Updates

201 The Multi-Layer Perceptron (MLP) component
202 serves as a position-wise feed-forward network that
203 processes each position independently, introducing
204 non-linearity and increasing the model's represen-
205 tational capacity. This component is crucial for
206 capturing complex patterns and transformations
207 that cannot be modeled by attention mechanisms
208 alone.

209 2.3.1 Standard Transformer MLP

210 The MLP block in this transformer architecture pro-
211 cesses the input hidden state x through a sequence
212 of operations. First, the input is normalized using
213 RMSNorm:

$$214 \quad \hat{x} = \text{RMSNorm}(x) \quad (13)$$

215 The normalized input is then projected through a
216 single expansion matrix to a higher-dimensional
217 space:

$$218 \quad z = \hat{x}W_1 \quad (14)$$

219 where $W_1 \in \mathbb{R}^{d \times 4d}$ expands the representation
220 to four times the model dimension. This ex-
221 panded representation is processed through the
222 SiLU (Elfwing et al., 2018) activation function:

$$223 \quad h = \text{SiLU}(z) = z \cdot \sigma(z) \quad (15)$$

where $\sigma(z)$ is the sigmoid function. Finally, the activated representation is projected back to the original dimension through a second linear transformation:

$$y = hW_2 \quad (16)$$

where $W_2 \in \mathbb{R}^{4d \times d}$. Unlike more complex variants, this implementation uses a straightforward structure without gating mechanisms, focusing on dimensional expansion and contraction through the two linear transformations with the SiLU activation providing non-linearity. The complete transformation can be summarized as:

$$\text{MLP}(x) = \text{SiLU}(xW_1)W_2 \quad (17)$$

This MLP operates within a residual framework in the transformer block, where its output is added to the input:

$$x = x + \text{MLP}(\text{RMSNorm}(x)) \quad (18)$$

2.3.2 N-transformer MLP

The N-transformer introduces crucial modifications to the MLP block by incorporating scaled updates and normalized computations. Unlike the standard transformer, this variant operates directly on the input without an initial RMSNorm layer when in N-transformer mode. The computation begins with a scaled intermediate representation:

$$UV = s_{uv} \cdot W_1 x \quad (19)$$

The scaling factor s_{uv} is carefully initialized and learned during training:

$$s_{uv} = s_{\text{init}} \cdot \frac{1}{s_{\text{scale}}} \cdot \sqrt{D} \quad (20)$$

where s_{init} is set to 1.0 and s_{scale} is the initialization scaling factor. This scaling ensures that the intermediate activations remain in a controlled range, particularly important given the expansion factor of the feed-forward layer. The expanded representation is then split into two components:

$$u, v = \text{split}(UV) \quad (21)$$

where both u and v are in \mathbb{R}^{4d} . These components interact through a SiLU activation:

$$x_{\text{mlp}} = u \odot \text{SiLU}(v) \quad (22)$$

The final projection is computed through:

$$h_{\text{mlp}} = W_2 x_{\text{mlp}} \quad (23)$$

A key distinction of the N-transformer lies in its update mechanism. Instead of a simple residual connection, it employs a normalized update:

$$\alpha = |\alpha_{\text{mlp}}| \cdot \frac{\alpha_{\text{init}}}{\alpha_{\text{scale}}} \quad (24)$$

where α_{mlp} is a learned parameter, α_{init} is 0.05, and α_{scale} is the base scaling factor. The final output is computed through a normalized interpolation. Let's define the normalization operator $\mathcal{N}(x)$ that performs L2 normalization:

$$\mathcal{N}(x) = \frac{x}{\|x\|_2} \quad (25)$$

Then the final update equation becomes:

$$x_{\text{out}} = \mathcal{N}(\mathcal{N}(x) + \alpha(\mathcal{N}(h_{\text{mlp}}) - \mathcal{N}(x))) \quad (26)$$

More concisely, if we let $\hat{x} = \mathcal{N}(x)$ and $\hat{h}_{\text{mlp}} = \mathcal{N}(h_{\text{mlp}})$:

$$x_{\text{out}} = \mathcal{N}(\hat{x} + \alpha(\hat{h}_{\text{mlp}} - \hat{x})) \quad (27)$$

This normalization-based update ensures that the network maintains stable gradients and controlled feature magnitudes throughout training, while the learned scaling factors allow the model to adaptively adjust the influence of the MLP transformation at each layer.

2.4 Residual Updates

The N-transformer introduces a novel approach to residual connections that fundamentally differs from the standard additive skip connections. Let $x \in \mathbb{R}^{B \times T \times D}$ be the input to a layer and $h \in \mathbb{R}^{B \times T \times D}$ be the transformed representation (either from self-attention, cross-attention, or MLP). The residual update is computed as follows: First, we define the L2 normalization function for any vector v :

$$\mathcal{N}(v) = \frac{v}{\|v\|_2} \quad (28)$$

The residual update in the N-transformer then becomes:

$$x_{\text{out}} = \mathcal{N}\left(\mathcal{N}(x) + \alpha \cdot (\mathcal{N}(h) - \mathcal{N}(x))\right) \quad (29)$$

where:

α is a learnable parameter initialized to a small value $\mathcal{N}(x)$ and $\mathcal{N}(h)$ are the L2-normalized input and transformed representations. The difference term $(\mathcal{N}(h) - \mathcal{N}(x))$ represents the update direction in normalized space. The outer normalization ensures the final output maintains unit norm.

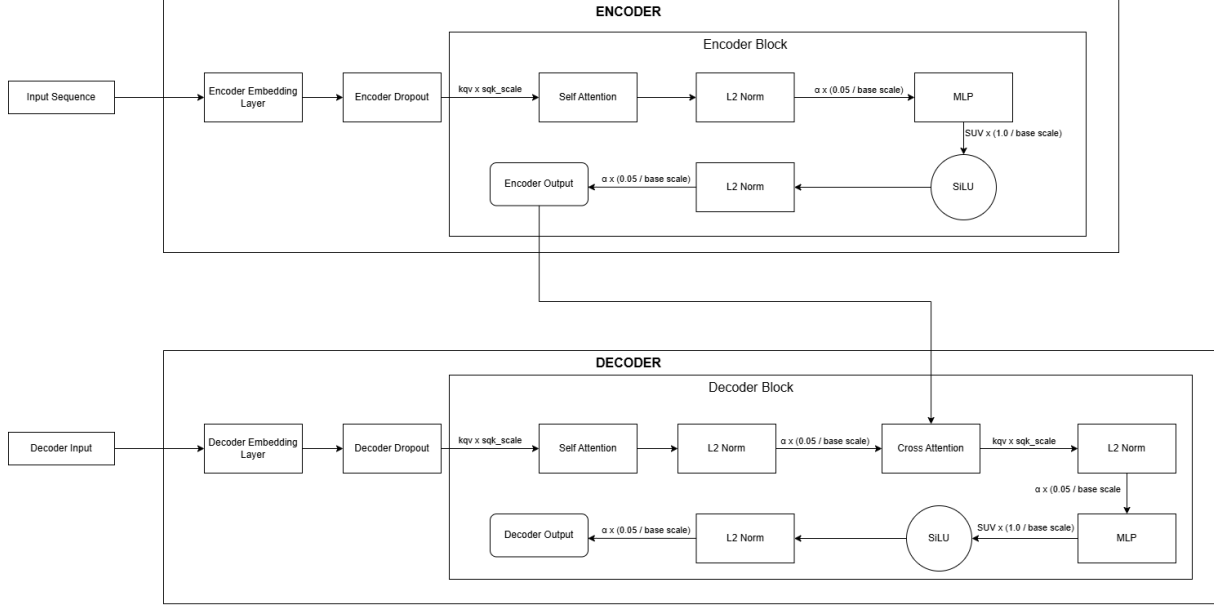


Figure 1: Architecture diagram of the N-transformer model.

This formulation can be interpreted as a form of spherical linear interpolation between normalized representations, with α controlling the magnitude of the update. The key advantages of this approach are:

- **Scale Invariance:** All operations occur in normalized space, making the updates independent of the magnitude of the input representations.
- **Controlled Updates:** The learned α parameter allows the model to adaptively determine the optimal interpolation between input and transformed representations.
- **Stability:** The double normalization ensures that the residual path maintains consistent scales throughout the network.
- **Gradient Flow:** The normalized difference provides a well-conditioned gradient path, potentially improving optimization.

α is typically initialized to a small value and is allowed to adapt during training, enabling the model to learn the optimal balance between preserving input information and incorporating transformations.

2.5 Comparison: Transformer vs. Normalized Transformer

In the normalized Transformer, all matrices and embeddings are normalized along their embedding dimension after each batch pass. The hidden state

updates are controlled by learnable vectors of eigen learning rates α_A and α_M .

| Model | Block Size | Validation Loss |
|----------------------------|------------|-----------------|
| Baseline transformer | 1024 | 4.54303 |
| Baseline transformer(GELU) | 1024 | 4.31210 |
| Baseline transformer | 512 | 4.50281 |
| N-transformer | 1024 | 4.28749 |
| N-transformer(GELU) | 1024 | 4.33878 |
| N-transformer | 512 | 4.38358 |

Table 2: Validation loss at 500 iterations for different models and block sizes.

3 Experiments

We begin by pre-training both the baseline Transformer and the normalized Transformer on the OpenWebText (Gokaslan et al.) dataset using the sequence-to-sequence objective and evaluate them on a set of standard downstream tasks. We experiment with medium-sized models with the N-transformer having 325.24 million parameters and the baseline transformer having 333.93 million parameters, including embeddings. A detailed description of the setup and hyperparameters is in Appendix A.1.

We evaluate our models on the GLUE benchmark (Wang, 2018), following the approach of (Raffel et al., 2020). Since the original test sets are not publicly available, we adopt the data split strategy proposed by (Zhang et al., 2020). For smaller datasets (RTE, MRPC) with fewer than 10K samples, we divide the original validation set

307
308
309
310
311

312
313
314
315

316
317
318
319

320
321
322

323
324
325

326
327
328
329

330
331

332
333
334

335
336
337

338

339

340
341
342
343
344
345
346
347
348
349
350
351
352
353
354
355
356
357
358

359 equally into validation and test sets. For larger
 360 datasets, we create a validation set by reserving
 361 1K samples from the training data and use the
 362 original validation set for testing. The same
 363 approach is applied to the WiC (Pilehvar and
 364 Camacho-Collados, 2018) and BoolQ (Clark et al.,
 365 2019) datasets from the SuperGLUE (Wang et al.,
 366 2019) benchmark. For the MNLI task, we report
 367 results on the MNLI matched dataset. We fine-tune
 368 both N-transformer and the baseline transformer
 369 models on downstream tasks for 100 iterations
 370 each, using a batch size of 64. Our results indicate
 371 a significant performance improvement of the
 372 N-transformer over the baseline transformer,
 373 with an average performance gain of 21%. All
 374 experiments were run on a single NVIDIA A100
 375 40GB GPU.
 376

377 4 Results

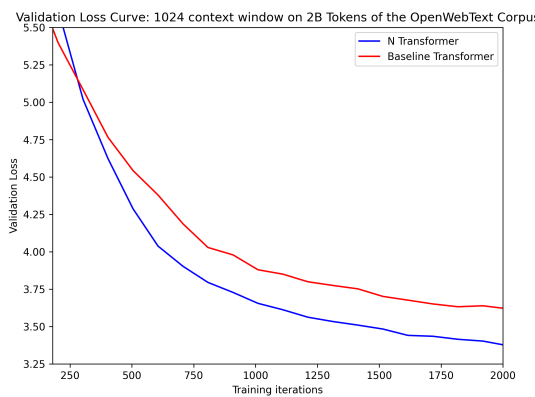
378 4.1 Analysis

379 The eigen learning rate distributions in Figure
 380 3 reveal fundamental differences in learning
 381 dynamics between encoder and decoder com-
 382 ponents. The decoder components demon-
 383 strate significantly higher learning rates, with attention
 384 rates ranging from 0.125 to 0.27 and MLP rates
 385 from 0.18 to 0.237, compared to the encoder’s
 386 more conservative rates of 0.021-0.039 for
 387 attention and 0.016-0.032 for MLP layers. This
 388 substantial disparity (approximately 5-10x) in
 389 learning rates between encoder and decoder
 390 components suggests a more aggressive learning
 391 strategy in the decoder, aligning with its role in
 392 generating diverse outputs. The encoder’s attention
 393 mechanism shows a gradual increase in learning
 394 rates across layers (0.0213 to 0.039), indicating
 395 progressively finer adaptation in deeper layers,
 396 while maintaining overall conservative updates. In
 397 contrast, the decoder’s attention exhibits higher
 398 initial learning rates that decrease in later layers
 399 (0.27 to 0.125), suggesting more aggressive
 400 learning in early layers followed by refinement.
 401 Notably, MLP learning rates in both components
 402 display more stable patterns than their attention
 403 counterparts, with decoder MLP rates maintain-
 404 ing consistently higher values (around 0.22) com-
 405 pared to encoder MLP rates (around 0.02). This stability
 406 in MLP rates, coupled with the more variable
 407 attention rates, indicates a well-structured learning
 408 process where feature transformation remains

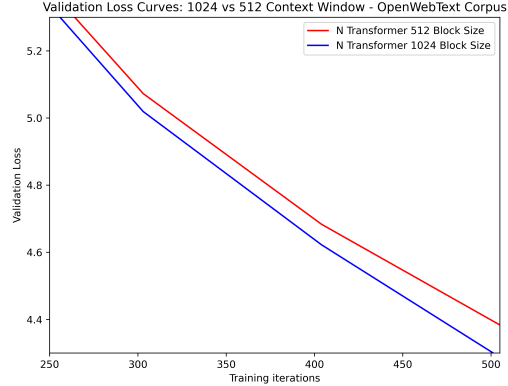
409 consistent while attention mechanisms adapt more
 410 dynamically based on their position and role in the
 411 network. Figure 2a shows the comparison
 412 of the validation loss between the N-transformer
 413 and the baseline transformer with a context
 414 window of 1024 and impact with block size. The
 415 N-transformer model achieves a lower validation
 416 loss (3.37) than the baseline transformer model
 417 (3.62). Figure 2b depicts that using a larger context
 418 window of 1024 shows a lower validation loss at
 419 500 iterations compared to a context window of
 420 512 for the N-transformer. Figure 4 provides an
 421 analysis of the scaling factors after pre-training the
 422 N-transformer model on the OpenWebText dataset.
 423 The scaling factors reveal distinct operational
 424 patterns across the encoder-decoder architecture.
 425 The decoder’s attention scaling (sqk) demon-
 426 strates a notable monotonic decrease from 0.28 to 0.142
 427 across layers, indicating a progressive refine-
 428 ment of attention focus as information flows deeper
 429 into the network. This contrasts sharply with
 430 the encoder’s attention scaling, which maintains
 431 consistently low values (0.026-0.039), suggesting
 432 more focused attention processing throughout.
 433 The feed-forward network scaling factors (su, sv)
 434 exhibit remarkable stability in both components,
 435 with decoder values slightly above unity (1.02-
 436 1.05) indicating minor feature amplification, while
 437 encoder values remain marginally below unity
 438 (0.98-0.99), suggesting subtle feature dampening.
 439 This dichotomy in scaling behavior, particularly
 440 in the attention mechanisms, aligns with the
 441 theoretical understanding of encoder-decoder
 442 architectures, where encoders focus on creating
 443 precise contextual representations while decoders
 444 progressively refine their attention from broad
 445 context consideration to specific token generation.
 446 The stability of feed-forward scaling factors
 447 across all layers indicates robust gradient flow
 448 and effective normalization, while the systematic
 449 difference between encoder and decoder scaling
 450 suggests specialized roles in sequence processing.

| Parameter | N-transformer | Baseline Transformer |
|--|-------------------------------------|-------------------------------------|
| Number of Encoder Layers (n_{layers}) | 6 | 6 |
| Number of Decoder Layers (n_{layers}) | 6 | 6 |
| Model Dimension (d_{model}) | 1024 | 1152 |
| Number of Attention Heads (n_{heads}) | 8 | 8 |
| Key Dimension (d_k) | $d_{\text{model}}/n_{\text{heads}}$ | $d_{\text{model}}/n_{\text{heads}}$ |
| MLP Dimension (d_{MLP}) | $4d_{\text{model}}$ | $4d_{\text{model}}$ |
| Total Parameters | 325.24M | 333.94M |

Table 3: Architectural configurations of N-transformer and Baseline Transformer models.



(a) Validation Loss Curve for 1024 Context Window



(b) Validation Loss Curve Comparison between context windows

Figure 2: Figure 2a: Validation loss curve comparing N-transformer and Baseline Transformer models with a 1024 context window. Figure 2b: Validation loss curves comparing N-transformer models with 512 and 1024 context window

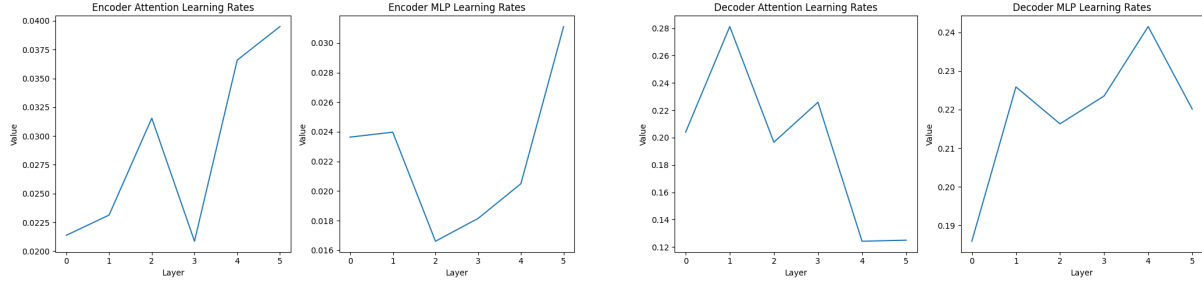


Figure 3: Layer-wise distribution of eigen learning rates across encoder and decoder components, illustrating distinct learning dynamics between attention and MLP layers, with decoder components exhibiting substantially higher learning rates compared to their encoder counterparts.

453 4.2 Downstream Tasks Results

454 We evaluate N-transformer and the Baseline trans-
 455 former on the GLUE Benchmark and WiC and
 456 BoolQ from the SuperGLUE benchmark. The N-
 457 transformer model exhibits an average increase
 458 in performance by **11.96%** after training for only
 459 about 100 iterations. This result shows the increase
 460 in convergence speed of the N-transformer in vari-
 461 ous language modeling tasks.

462 5 Conclusion

463 This work builds on important artifacts and find-
 464 ings made by NVIDIA in their report 'nGPT' and
 465 presents a novel encoder-decoder architecture that
 466 leverages hyperspherical normalization and adap-
 467 tive scaling factors. Through careful analysis of
 468 the scaling factors and eigen learning rates, we
 469 observe distinct behavioral patterns between en-
 470 coder and decoder components that provide in-
 471 sights into the model's learning dynamics. The

472 decoder's attention scaling factors show a progres-
 473 sive focusing behavior, while maintaining stable
 474 feed-forward scaling slightly above unity, indicat-
 475 ing effective feature amplification. In contrast, the
 476 encoder maintains consistently low attention scal-
 477 ing with feed-forward values slightly below unity,
 478 suggesting precise contextual representation learn-
 479 ing. These patterns are complemented by the eigen
 480 learning rate distributions, where decoder compo-
 481 nents exhibit significantly higher rates compared
 482 to encoder components, enabling more aggressive
 483 learning in the decoding phase while maintain-
 484 ing stable feature transformations. The effectiveness
 485 of this architecture is demonstrated by its substan-
 486 tial performance improvement of 11.96% over the
 487 baseline transformer on GLUE and SuperGLUE
 488 benchmarks.

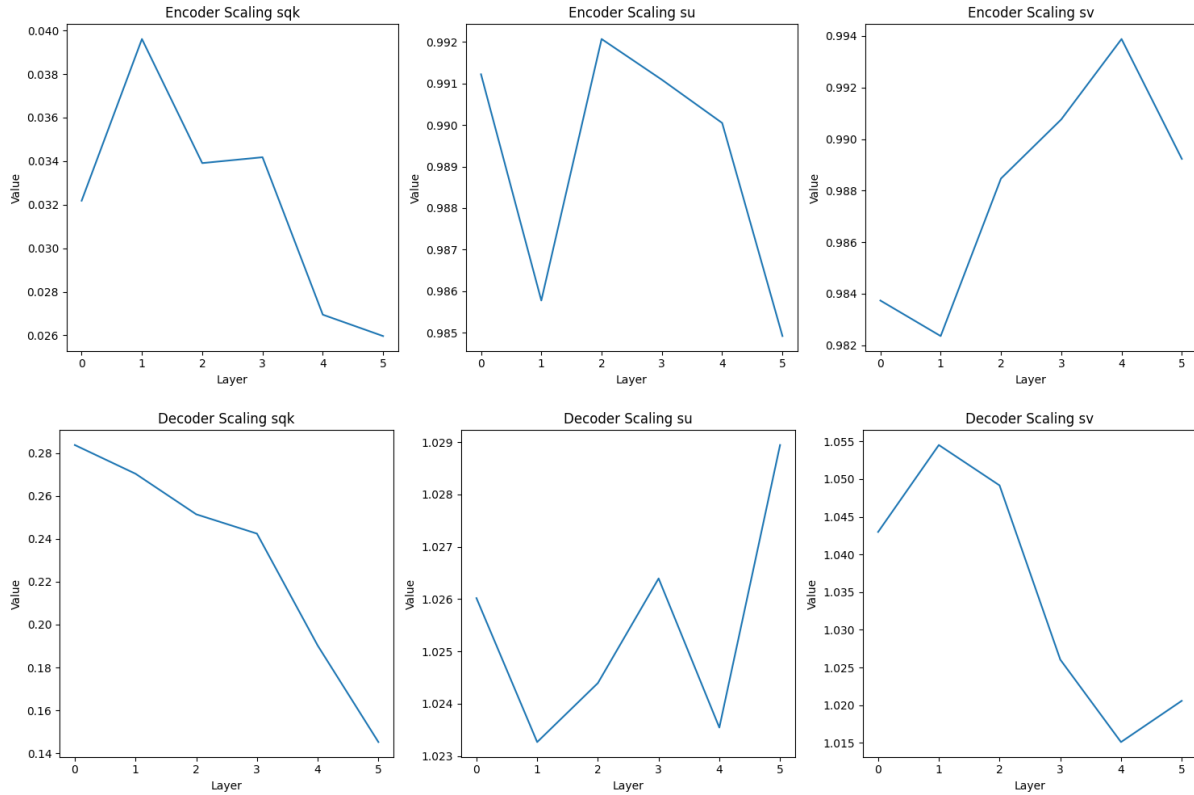


Figure 4: Evolution of scaling factors across encoder and decoder layers (0-5) of the N-transformer, showing distinct patterns between attention (sqk) and feed-forward (su, sv) components.

| Model | MRPC (Acc / F1) | QNLI | QQP (Acc / F1) | RTE | MNLI | SST-2 | BoolQ | WiC | Overall Avg. |
|---------------|----------------------|--------------|----------------------|--------------|--------------|--------------|--------------|--------------|--------------|
| Transformer | 61.54 / 71.43 | 56.12 | 72.45 / 52.94 | 49.31 | 33.38 | 77.84 | 63.66 | 51.72 | 59.04 |
| N-Transformer | 61.54 / 69.47 | 62.72 | 79.31 / 69.92 | 56.94 | 57.31 | 80.00 | 66.07 | 57.66 | 66.10 |

Table 4: Performance comparison between Transformer and N-transformer across multiple datasets. Scores for MRPC, QQP, and MNLI are reported as (Accuracy / F1), while other datasets display accuracy. Overall Avg. represents the average performance across all datasets. The N-transformer model exhibits an average increase in performance by 11.96% after training for 100 iterations with a batch size of 64

6 Limitations

While the N transformer demonstrates promising results in terms of early learning capabilities and performance improvements, several limitations must be acknowledged. The most significant drawback is the computational overhead introduced by the double normalization process, which increases each training step’s duration by approximately 80%. This substantial overhead presents challenges for scaling the architecture to larger models or longer training durations. Additionally, the current implementation should be viewed primarily as a proof of concept for a novel training paradigm rather than a direct competitor to established architectures on downstream tasks, as it has only undergone limited

pre-training iterations.

Future work could address these limitations in several directions. First, optimizing the normalization computations through techniques like fused operations or adaptive normalization schedules could potentially reduce the computational overhead. Second, scaling the N transformer to larger network sizes and evaluating its performance on real-world datasets would provide valuable insights into its practical applicability. The architecture could be extended by exploring adaptive scaling mechanisms that dynamically adjust based on layer depth and attention patterns, or by investigating hybrid normalization schemes that balance computational efficiency with representational power. An extension of the architecture towards hybrid ar-

chitectures (Dao and Gu, 2024) is straightforward. Furthermore, investigating the integration of sparse attention mechanisms or conditional computation paths could enhance the model’s efficiency while maintaining the benefits of hyperspherical normalization. The promising early learning behavior also suggests potential applications in few-shot learning scenarios, where rapid adaptation is crucial.

References

- Jimmy Lei Ba. 2016. Layer normalization. *arXiv preprint arXiv:1607.06450*.
- Christopher Clark, Kenton Lee, Ming-Wei Chang, Tom Kwiatkowski, Michael Collins, and Kristina Toutanova. 2019. Boolq: Exploring the surprising difficulty of natural yes/no questions. *arXiv preprint arXiv:1905.10044*.
- Francesco D’Angelo, Maksym Andriushchenko, Aditya Varre, and Nicolas Flammarion. 2023. Why do we need weight decay in modern deep learning? *arXiv preprint arXiv:2310.04415*.
- Tri Dao and Albert Gu. 2024. Transformers are ssms: Generalized models and efficient algorithms through structured state space duality. *arXiv preprint arXiv:2405.21060*.
- Stefan Elfwing, Eiji Uchibe, and Kenji Doya. 2018. Sigmoid-weighted linear units for neural network function approximation in reinforcement learning. *Neural networks*, 107:3–11.
- Aaron Gokaslan, Vanya Cohen, E Pavlick, and S Tellec. Openwebtext corpus. 2019. URL <http://Skylion007.github.io/OpenWebTextCorpus>, page 9.
- Maxim Kodryan, Ekaterina Lobacheva, Maksim Nakhodnov, and Dmitry P Petrov. 2022. Training scale-invariant neural networks on the sphere can happen in three regimes. *Advances in Neural Information Processing Systems*, 35:14058–14070.
- I Loshchilov. 2017. Decoupled weight decay regularization. *arXiv preprint arXiv:1711.05101*.
- Ilya Loshchilov, Cheng-Ping Hsieh, Simeng Sun, and Boris Ginsburg. 2024. ngpt: Normalized transformer with representation learning on the hyper-sphere. *arXiv preprint arXiv:2410.01131*.
- Mohammad Taher Pilehvar and Jose Camacho-Collados. 2018. Wic: the word-in-context dataset for evaluating context-sensitive meaning representations. *arXiv preprint arXiv:1808.09121*.
- Colin Raffel, Noam Shazeer, Adam Roberts, Katherine Lee, Sharan Narang, Michael Matena, Yanqi Zhou, Wei Li, and Peter J Liu. 2020. Exploring the limits of transfer learning with a unified text-to-text transformer. *Journal of machine learning research*, 21(140):1–67.
- Tim Salimans and Durk P Kingma. 2016. Weight normalization: A simple reparameterization to accelerate training of deep neural networks. *Advances in neural information processing systems*, 29.
- Jianlin Su, Murtadha Ahmed, Yu Lu, Shengfeng Pan, Wen Bo, and Yunfeng Liu. 2024. Roformer: Enhanced transformer with rotary position embedding. *Neurocomputing*, 568:127063.
- Ashish Vaswani, Noam Shazeer, Niki Parmar, Jakob Uszkoreit, Llion Jones, Aidan N Gomez, Łukasz Kaiser, and Illia Polosukhin. 2017. Attention is all you need. In *Advances in Neural Information Processing Systems*, volume 30.
- Alex Wang. 2018. Glue: A multi-task benchmark and analysis platform for natural language understanding. *arXiv preprint arXiv:1804.07461*.
- Alex Wang, Yada Pruksachatkun, Nikita Nangia, Amanpreet Singh, Julian Michael, Felix Hill, Omer Levy, and Samuel Bowman. 2019. SuperGLUE: A stickier benchmark for general-purpose language understanding systems. *Advances in neural information processing systems*, 32.
- Ruixin Xiong, Yunchang Yang, Di He, Kai Zheng, Shuxin Zheng, Chen Xing, Huishuai Zhang, Yanyan Lan, Liwei Wang, and Tieyan Liu. 2020. On layer normalization in the transformer architecture. In *International Conference on Machine Learning*, pages 10524–10533. PMLR.
- Biao Zhang and Rico Sennrich. 2019. Root mean square layer normalization. *Advances in Neural Information Processing Systems*, 32.
- Tianyi Zhang, Felix Wu, Arzoo Katiyar, Kilian Q Weinberger, and Yoav Artzi. 2020. Revisiting few-sample bert fine-tuning. *arXiv preprint arXiv:2006.05987*.

A Appendix

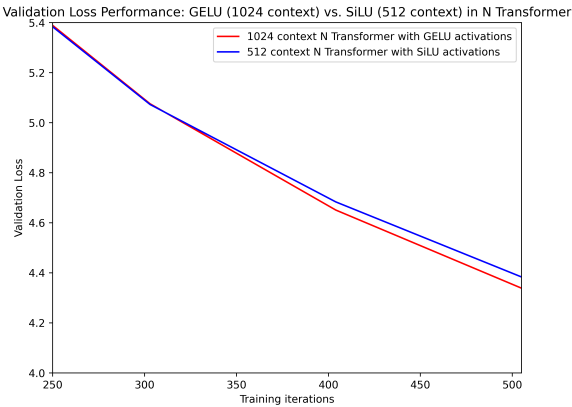


Figure 5: Validation loss curves comparing the N transformer with SiLU activations having a lower block size and an N transformer model using GELU activations having a higher block size on the OpenWebText dataset

A.1 Effect of SiLU in N transformer

Figure 5 demonstrates an intriguing relationship between activation functions and context length in N-transformer architectures. The validation loss curves show that an N-transformer using SiLU activations with a 512-token context length achieves comparable performance to one using GELU activations with a 1024-token context length, with only a marginal difference in validation loss (approximately 0.05 higher for SiLU across iterations). This finding is particularly significant given the model architecture's use of normalized attention mechanisms and residual pathways. The SiLU activation $\sigma(x) \cdot x$ in the feed-forward network, combined with the model's normalization scheme, appears to compensate for the reduced context length, suggesting that the choice of activation function can have architectural implications beyond simple non-linearity. The convergence patterns indicate that while both variants show consistent improvement over training iterations (250-500), the GELU variant with longer context maintains a slight edge in final performance (validation loss of 4.33 vs 4.38). However, the computational efficiency gained from halving the context length while maintaining comparable performance could present a valuable trade-off, especially in resource-constrained environments.

A.2 Pre-training hyperparameter settings

| Parameter | N-transformer | Transformer |
|-----------------------------|------------------------------|---------------------|
| Batch Size | 16 | 16 |
| Dropout | 0.1 | 0.1 |
| Training Iterations | 2000 | 2000 |
| β_1 | 0.9 | 0.9 |
| β_2 | 0.95 | 0.95 |
| Learning Rate | 15×10^{-4} | 15×10^{-4} |
| Weight Decay | 0.0 | 0.1 |
| Warmup Iterations | 0 | 100 |
| Base Scale | $1.0/\sqrt{n_{\text{embd}}}$ | 0.02 |
| Encoder Layers | 6 | 6 |
| Decoder Layers | 6 | 6 |
| Model Dimension | 1024 | 1152 |
| Attention Heads | 8 | 8 |
| Block Size (Context Window) | 1024 | 1024 |
| Total Parameters | 325.24M | 333.94M |

Table 5: Comparison of hyperparameters between N-transformer and the Baseline Transformer.

Table 6: Comparison of architectural parameters between N-transformer and Baseline Transformer.

Table 6 describes the hyperparameter settings used for pre-training both the N transformer and the baseline transformer on the OpenWebText dataset with the sequence-to-sequence objective.

A.3 Downstream tasks results analysis

From Table 4, we can observe that the N transformer model outperforms the baseline transformer by wider margins on tasks with samples having longer sequences such as RTE, MNLI and QNLI and the performance gap narrows as the sequence lengths of the samples reduce as seen in MRPC, SST-2 and QQP tasks in the GLUE Benchmark. The performance patterns observed across different sequence lengths may be attributed to several

650 architectural features of the N transformer. The
651 model’s normalized attention mechanism, imple-
652 mented through L2 norm and carefully calibrated
653 scaling factors, appears to facilitate more stable gra-
654 dient flow in longer sequences. The architecture’s
655 approach to normalization may be particularly ben-
656 efitcial in maintaining consistent gradient magni-
657 tudes across varying sequence lengths, potentially
658 enabling better capture of long-range dependen-
659 cies. Interestingly, the narrowing performance gap
660 in tasks with shorter sequences, such as MRPC,
661 SST-2, and QQP, suggests that the benefits

662
663 of the normalization strategy might become more
664 pronounced as sequence length increases. This be-
665 havior could indicate that while the normalized ar-
666 chitecture provides advantages across all sequence
667 lengths, its impact is most notable in scenarios
668 requiring the model to process and maintain rela-
669 tionships over longer distances.